17.04.2005
WIS/07/05-APR-DPP

Search for RPV SUSY Through its Purely Hadronic Decay Modes With Low Luminosity at LHC

Ehud Duchovni and Arie Melamed-Katz [1]

Abstract

Two search procedures for signals of R-Parity Violating SUSY at ATLAS are proposed. The first one makes use of R-Parity Conserving production of a sparton pair followed by their RPV decay. The present procedure differs from previously proposed ones in two aspects: It does not require the presence of an identified lepton in the final state; and it makes use of b-tagging. The second channel is the resonating squark production through RPV coupling followed by its RPV decay into two quarks. Here also one can benefit from the use of b-tagging. The discovery potential of ATLAS in these two channels is evaluated.

[1]Particle Physics Department, Weizmann Institute of Science, Rehovot 76100, Israel.

1 Introduction

The sensitivity of the ATLAS experiment to R Parity Violating (RPV) SUSY signals through a pair production of sparticles by an RPC process, followed by RPV decay was investigated in a number of cases [1]-[7]. The simplest relevant Feynman diagram of such a process is depicted in Figure 1a. It was concluded (e.g. in the 'Detector and Physics Performance Technical Design Report' (TDR)) that SUSY RPV signal can be established if and only if leptons exist in the final state and are required by the signal selection procedure. Such a restriction is undesirable since one doesn't know which is the soft SUSY breaking mechanism, and how will the sparticle mass hierarchy look like. Consequently, one doesn't know how many leptons might be present in the various possible SUSY final states. In the present note it is shown that the existence of a SUSY RPV signal can be established using purely hadronic final states. The proposed search procedure might turn out to be a discovery channel if squarks and gluinos are lighter than sleptons and most of the gauginos. It is more likely to end up as a corroborating channel if the mass hierarchy of super particles turns out to be similar to the one expected by the leading contemporary SUSY models. The analysis procedure which is presented here differs from the one proposed in [1] mainly in one crucial aspect; it does not require a large number of jets. By significantly reducing the number of required jets, one lowers the systematics uncertainties on the estimated QCD background and enhances the reliability of the result. Another significant enhancement of the analysis discovery potential is achieved by requiring the presence of at least one b-flavored jet in the final state.

A second topic, namely, the resonating squark production through the s-channel as depicted schematically in Figure 1b is also discussed in the present note. Such a process is allowed once the 3-quark RPV coupling ($\lambda^{"}_{ijk}U^c_i D^c_j D^c_k$), where U and D are the up and down isosinglet quark superfields, differs from zero. This process leads to hadronic final states and was, to the best of our knowledge, never studied [2]. It is shown that ATLAS will have a significant discovery potential for this process, provided $\lambda^{"}_{ijk}$ is large, even with low integrated luminosity.

[2]Resonant production of slepton and stop at Tevatron were studied [8] only when leptonic final states were expected.

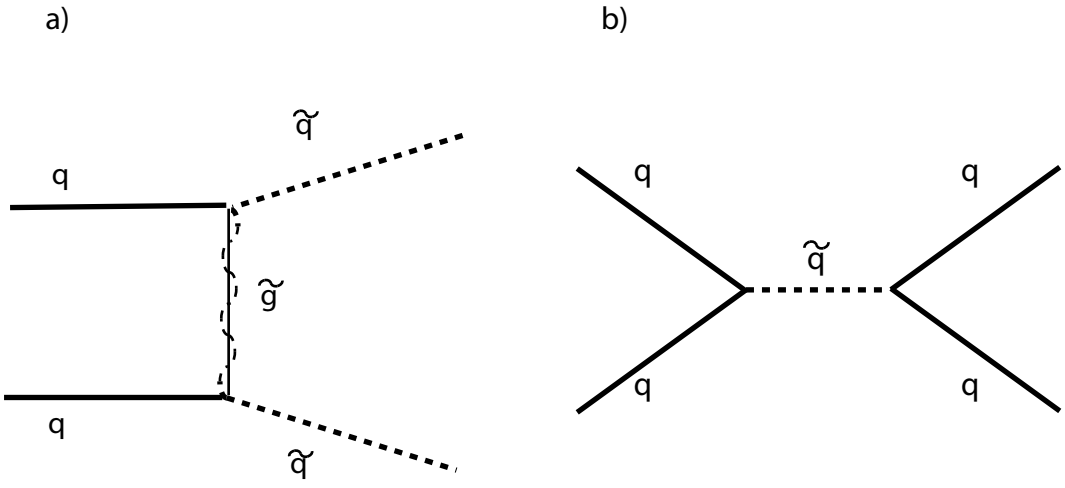

Figure 1: Two schematic examples of the relevant processes. Left (a) is the RPC pair production and on the right (b) is the resonant squark production.

2 Signal and Background Simulation

Signal for both processes was simulated by ISAWIG (version 1.105) followed by Herwig (version 6.4) [9] and the events were later pushed through the fast detector simulation program [3] of the ATLAS detector. 100K events have been generated at the TDR SUSY MSSM point #5 [4] and 1000 events at 70 other points in a grid along the relevant region in the $(m_0, m_{1/2})$ plane. Background was produced also using Herwig 6.4 and was pushed through the same simulation program. The various background processes that have been simulated are summarized in Table 1. In order to limit the number of required simulated events, a p_t cut at the production level was applied (column 3 in the table). A test verifying that this cut has a negligible effect on the results was carried out.

For the systematic uncertainty studies some signals were also simulated with Herwig 6.5 and the relevant background was simulated again using a different version of Herwig, namely, 6.5 as well as Pythia 6.157 [10]

[3] The Fortran version 2.53 was used.

[4] at this point $m_0 = 100$ GeV, $m_{1/2} = 300$ GeV, $A_0 = 300$ GeV, $tan\beta = 2.1$ and μ is taken to be positive.

Process	Herwig Proc #	p_t Range $[GeV]$	σ $[nb]$
QCD $2 \to 2$	1500	20-100	580,000
”	”	100-250	1,145
”	”	250-400	18.8
”	”	> 400	2.2
$q\bar{q} \to Z^0/\gamma \to q'\bar{q}'$	1300	> 20	48.3
$q\bar{q}' \to W^{\pm} \to q''\bar{q}'''$	1400	> 20	93.6
$\gamma + jet$	1800	> 20	132.7
$W + jet$	2100	> 20	32.7
$Z + jet$	2150	> 20	10.6
Photon exchange	2450	> 20	20.1

Table 1: The background processes which were simulated for the present study.

3 RPC Production of Sparton Pair

The production process of sparton pair, which is the process under study in this section, is the 'conventional' pair production one (e.g. Figure 1a). The RPV couplings are brought here into action only at the decay stage and give rise to decay modes with large transverse energy (since squarks and gluinos are expected to be fairly heavy [12]), and long cascade decay chains. While long cascade chains normally give rise to high jet multiplicity this feature is not a very good separator of signal from SM background since its simulation, in particular in QCD processes, suffers from large systematic uncertainty. Instead, the combination of high mass and long decay chains gives rise to events with spherical topology, which is exploited here as one of the main separators. Consequently the following cuts are applied:

1. $\Sigma p_t > 1200\ GeV$: where Σp_t is the scalar sum of transverse momenta of all the jets in the event [5];
2. $N_{jet} > 4$: where only jets with $|\eta| < 2.5$ and $p_t > 80\ GeV$ are counted;
3. $T < 0.80$: where T is the Thrust value;
4. $C > 0.15$: where C is the Circularity of the event.

[5]jets are defined here as clusters with minimal energy of 10 GeV and radius of R=0.4 in a pseudorapidity range between -5 and 5.

The first cut is required in order to reduce the bulk of low energy QCD background. Once this is done, and once the well simulated and obviously irrelevant low-jet multiplicity configurations are removed by requiring more than four jets (cut 2), one can turn into the topology cuts. The Thrust analysis is performed in 3D while the circularity is done in 2D. Hence, the correlation between these two measures of energy spread in the events is not trivial (Figure 2). The accumulated effect of these cuts is shown in Figure 3. The TDR cut on $p_t^{jet1} > 100\ GeV$, where p_t^{jet1} is the transverse momentum of the most energetic jet was found to be redundant due to the strong cut on Σp_t.

The remaining background after these cuts is dominated by QCD processes. The estimation of this background is difficult because of its huge production cross-section. In order to cope with this we have split the QCD simulation at the production stage into p_t bins. The high p_t region, namely, when $p_t > 200\ GeV$ was fully simulated with equivalent luminosity of $1fb^{-1}$. In the lower p_t region, where the cross section is very large, only few p_t bins were simulated and an interpolation followed by integration was preformed. Since the selection cuts that were listed above strongly prefer high p_t final states, QCD events which were produced with low production p_t almost never made it through the cuts. Consequently, the interpolation procedure of the simulation of the low p_t region resulted in a negligible systematic uncertainty.

Using this procedure and assuming an integrated luminosity of merely $1fb^{-1}$ one can evaluate the 5σ sensitivity coverage of the ATLAS detector.

In order to estimate the sensitivity coverage one must first compute the mass spectrum and the consequent production cross section and decay modes of the signal. This is done, as mentioned above, by ISAWIG which makes use of the standard MSSM mass spectrum. The underlying ISAWIG assumption is true as long as the relevant RPV coefficients ($\lambda"_{ijk}$) are smaller than ≈ 0.1. Once they are larger than this value their inclusion in the RGE equations induces sizable changes in the physical masses of the super symmetric particles. The correct computation in this case is done using SOFTSUSY [11]. The area in the $(m_0, m_{1/2})$ region of the MSSM parameter space in which a signal will be observable is shown in Figure 4 for two cases: for low $\lambda"$ [6] where the mass spectrum of sparticles is derived by ISAWIG; and for large $\lambda"$ (namely for $\lambda" \approx 1$), where the mass spectrum of sparticles is derived by SOFTSUSY. As one can see in Figure 4 the inclusion of RPV couplings leads to a significant change in

[6] a value of $\lambda = 0.004$ was used but the results are not sensitive to the exact value as long as it is below ≈ 0.1.

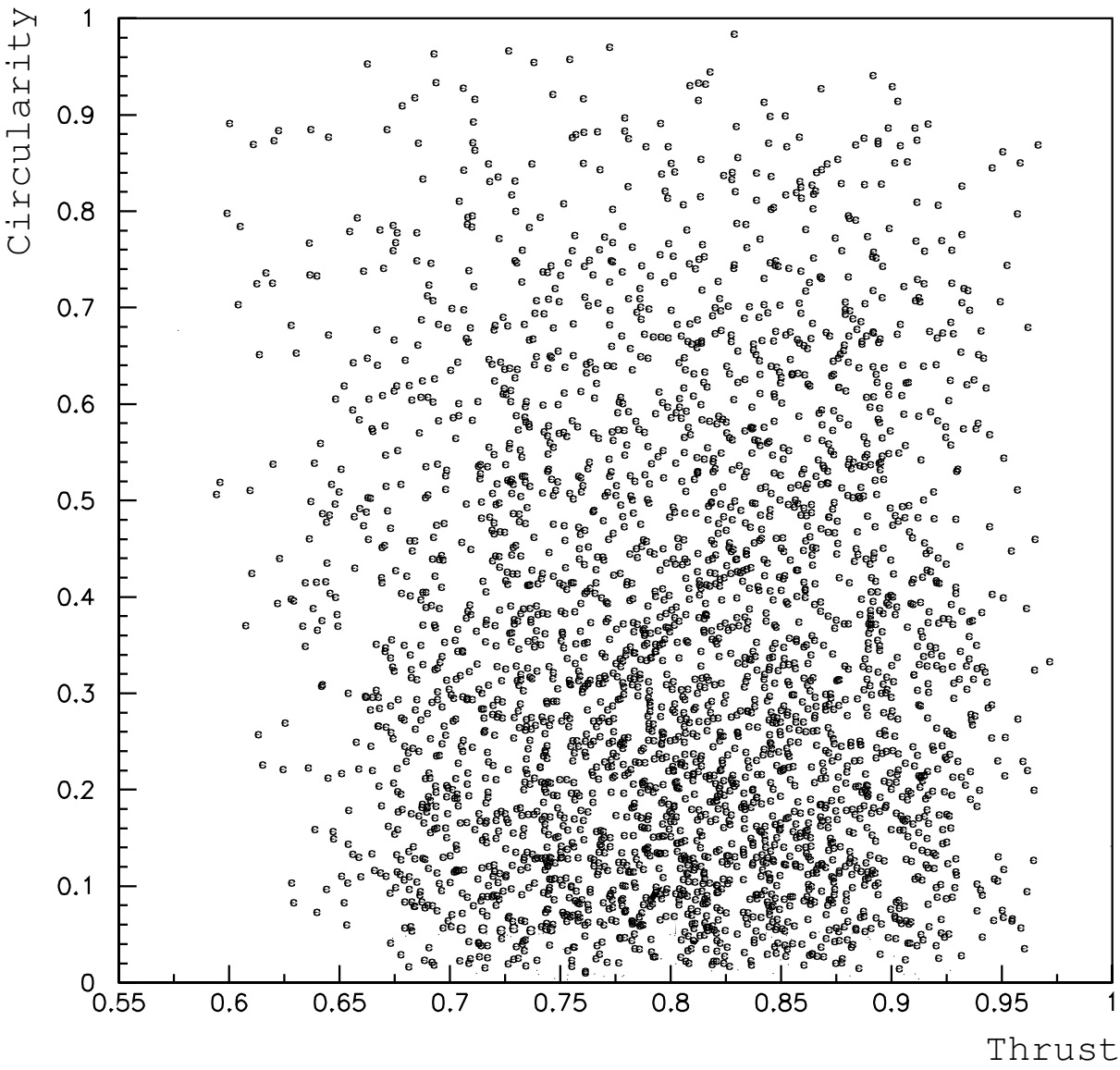

Figure 2: The correlation between the two-dimensional Circularity and the three dimensional Thrust in simulated signal events.

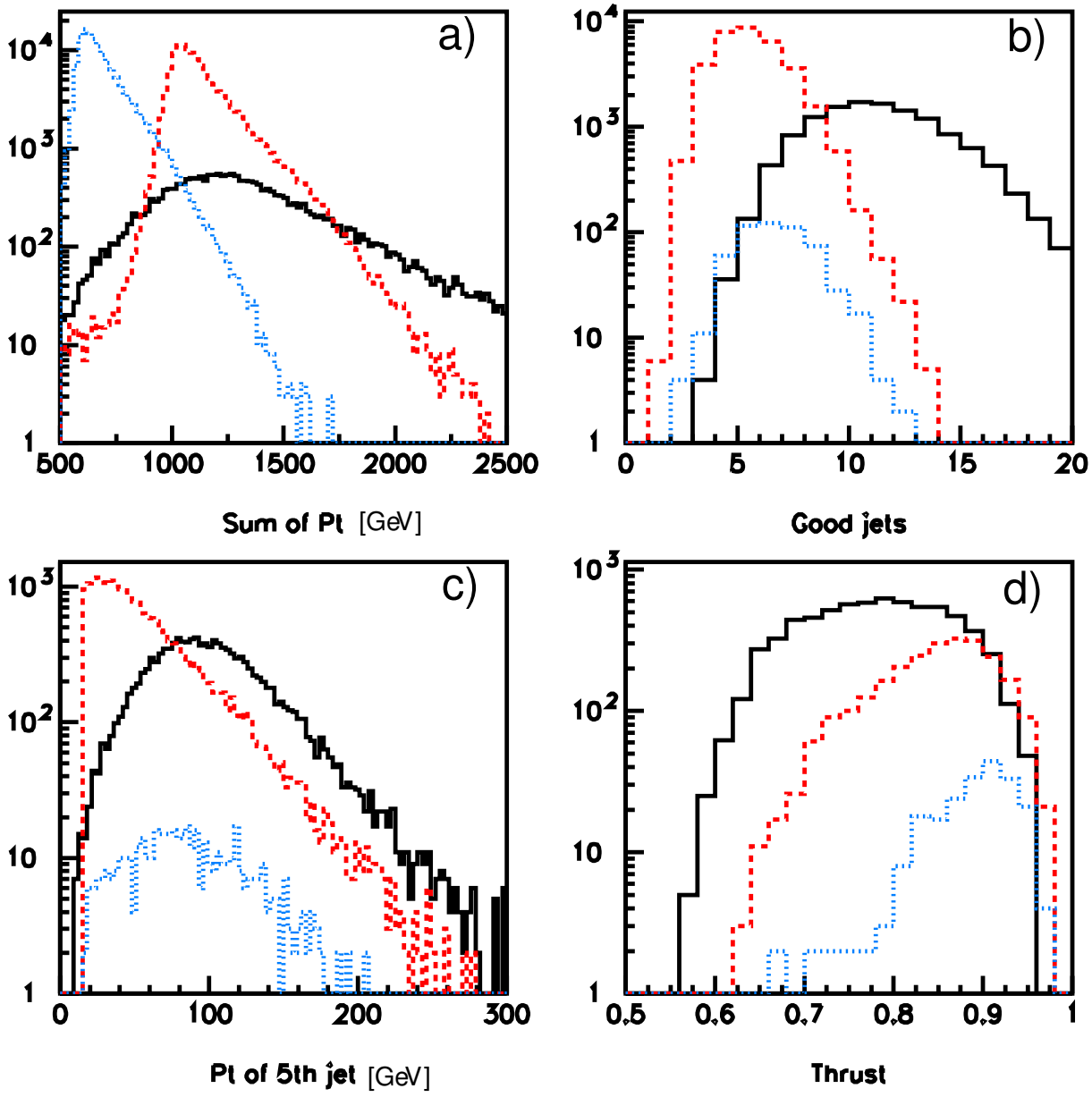

Figure 3: The accumulated effect of the analysis cuts: a) shows the Σp_t distribution for the signal at point #5 (solid black), QCD background simulated in the 300-301 GeV region (dotted blue) and QCD background in the 500-520 GeV region (dashed red) all curves are absolutely normalized to a luminosity of $1 fb^{-1}$; b) the distributions of the number of "good jets" (inside $|\eta| < 2.5$) after the $\Sigma p_t > 1200\ GeV$ cut is applied. c) The p_t of the 5^{th} jet after events with more than 4 "good jets" are selected; d) The Thrust after the cuts on the Circularity and the p_t of the 5^{th} jet have also been applied.

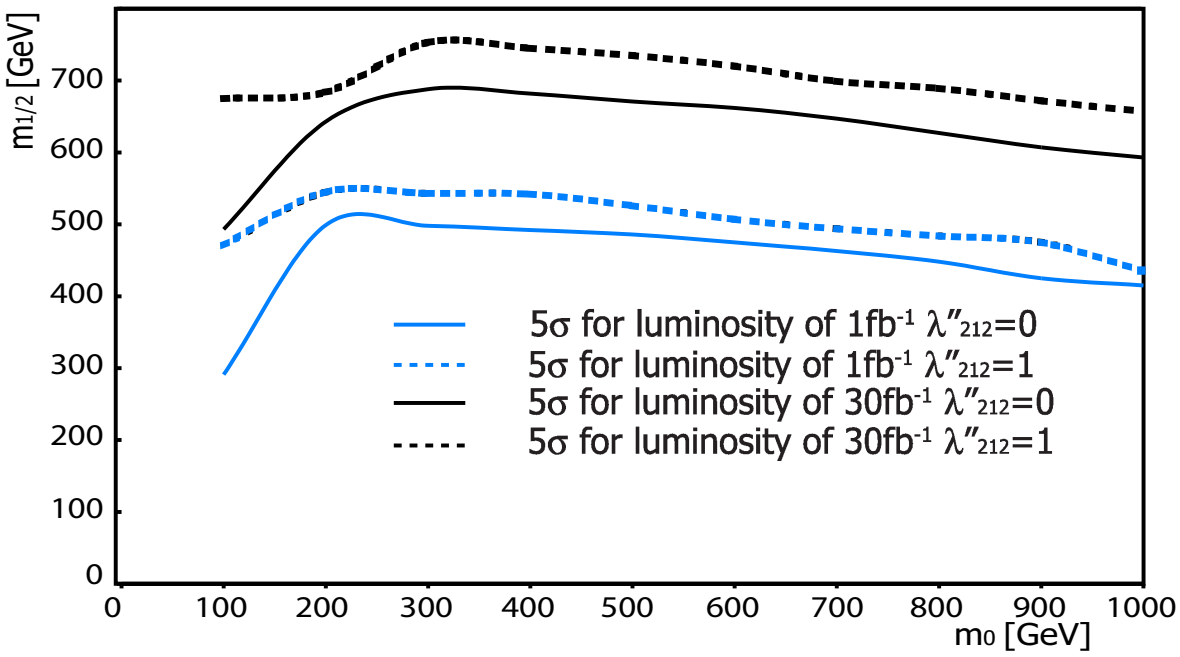

Figure 4: The sensitivity of ATLAS to RPV signal in the hadronic channel plotted in the $(m_0, m_{1/2})$ plane for two luminosities: 1 (blue) and 30 fb^{-1} (black), for $A_0 = 0$, $\mu > 0$, $tan\beta = 30$ and for two values of $\lambda"_{212}$: small, namely, 4×10^{-3} (solid curves) which coincides with standard computations, and large, namely, $\lambda"_{212} = 1$ (dashed curves) in which the effect of the inclusion of RPV couplings in the RGE equations is maximal [11]. The region below the curves can be explored by ATLAS.

the estimated sensitivity. For completeness, a curve showing the sensitivity with luminosity of $30fb^{-1}$ is also included. The sharp drop in sensitivity at low m_0 and low $\lambda"$ value results from the fact that under these conditions, due to the smallness of $\lambda"$ the RPC decays dominate and most of the events give rise to a stau which is, in this region, the LSP. Direct RPV decays of stau are not possible (since, as mentioned above, only $\lambda"_{ijk}$ are allowed to assume non zero values) in this scenario. Consequently the stau lifetime is long, the signal looks like an RPC one, and the present RPV oriented analysis has a low efficiency.

The efficiency of the procedure is also small in the low $(m_0, m_{1/2})$ region due to the hard Σp_t cut. However, the sensitivity is retained in this region since the low efficiency is compensated by the very large production cross section.

3.1 b-tagging

The sensitivity of the present search can be enhanced considerably by requiring the presence of b-flavored jets in the final state of the selected events. The percentage of b-flavored jets can approach 50% even for the case in which $\lambda"_{112}$ or $\lambda"_{212}$ differ from zero, as is the case for point #5 which is presented in Table 2.

Coupling	b Content
$\lambda"_{113}$	98%
$\lambda"_{123}$	98%
$\lambda"_{213}$	98%
$\lambda"_{223}$	98%
$\lambda"_{312}$	64%
$\lambda"_{313}$	61%
$\lambda"_{323}$	55%
$\lambda"_{112}$	45%
$\lambda"_{212}$	45%

Table 2: The fraction of true b-flavored events in RPV events at point #5.

The fact that even $\lambda"_{212}$ and $\lambda"_{112}$ give rise to final states rich in b-quarks might be considered as a surprise. However, a closer look reveals that those b-quarks originate mainly from $\tilde{g} \to \chi_1^0 q\bar{q}$ and $\tilde{g} \to \chi_1^{\pm} q\bar{q}'$ decays when $m_{1/2}$ is low. For higher values of $m_{1/2}$ the yield of b-quarks increases due to the opening of the direct $\tilde{g} \to \tilde{b}\bar{b}$ or $\tilde{g} \to \tilde{t}\bar{t}$ decays. For even higher values of $m_{1/2}$ the abundance of b-quarks drops due to the closure of the $\tilde{q} \to \tilde{g}q$ channel, which leads to a depletion in the number of $\tilde{g}$ that can decay into b-flavored quarks. The percentage of b-flavored events as a function of m_0 and $m_{1/2}$ for the case of $\lambda"_{212} = 1$ is shown in Figure 5.

For illustrative purposes a simple approximation for the b-tag capabilities of ATLAS was adopted in conducting the following study: b-flavored jets were assumed to be tagged, in the $|\eta| < 2.5$ region provided their transverse momentum exceeds 15 GeV, with efficiency of 50% and similar non-b-flavored jets were assumed to have a probability of 0.43% to be wrongly identified as b-tagged jets. No p_t or η dependence of these parameters was assumed. Under these simplistic assumptions one finds that the sensitivity of ATLAS for e.g. $\lambda"_{123}$ is improved significantly as is shown in Figure 6.

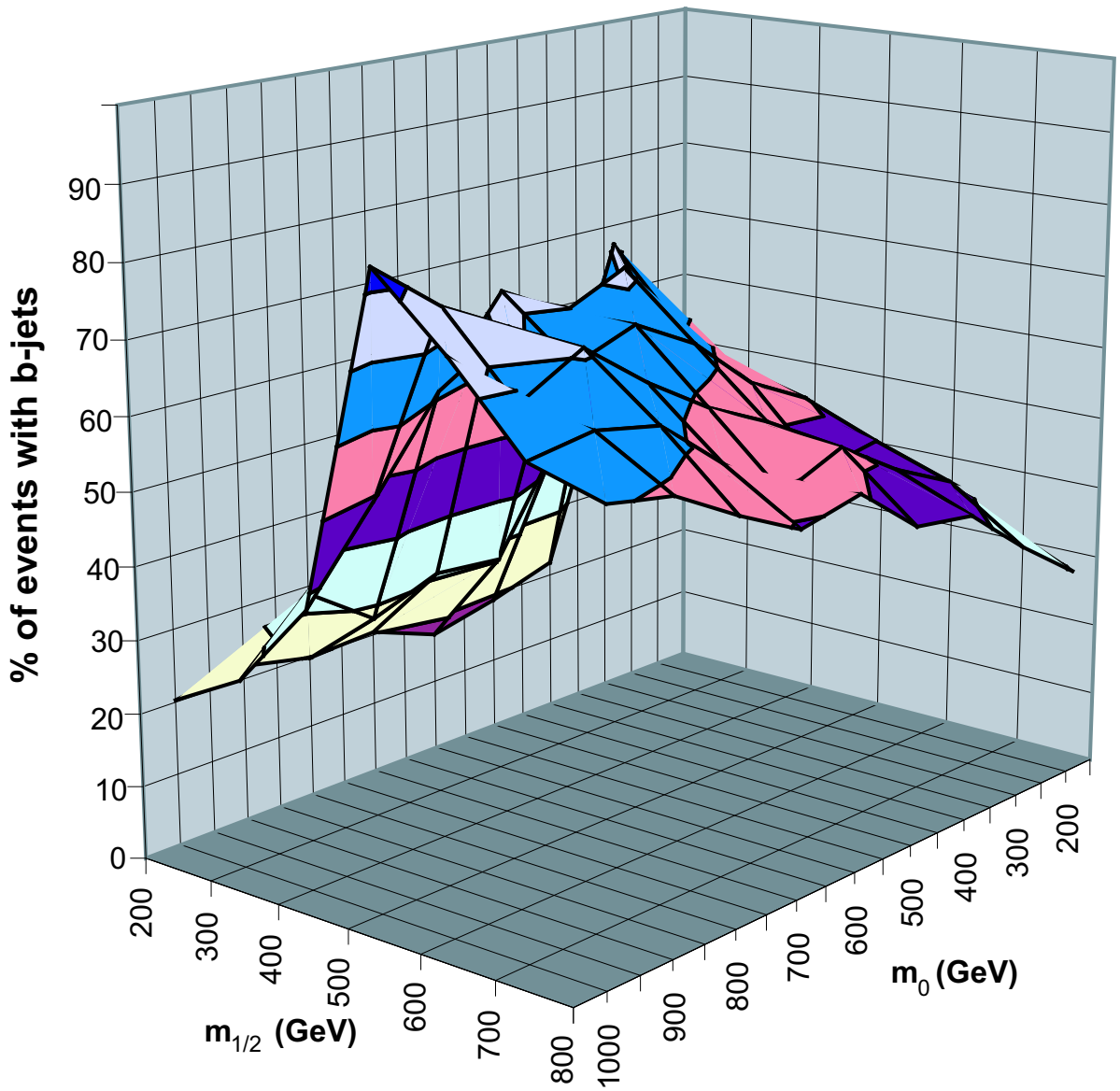

Figure 5: The percentage of b-flavored events in SUSY events as a function of m_0 and $m_{1/2}$ for the case of $\lambda"_{212} = 1$, $A_0 = 0$, positive μ and $tan\beta = 10$.

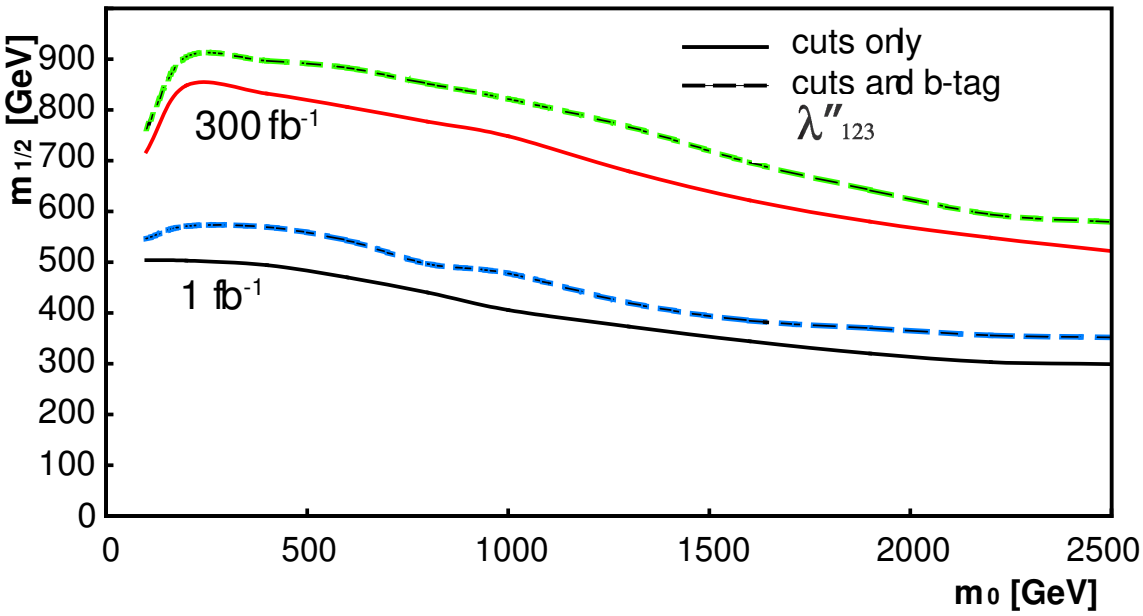

Figure 6: The sensitivity of ATLAS to RPV signal in the hadronic channel plotted in the $(m_0, m_{1/2})$ plane for two luminosities: 1 and 300 fb^{-1} for $\lambda"_{123}$. The dashed lines (upper (green) for luminosity of $300 fb^{-1}$ and lower (blue) for $1 fb^{-1}$) indicates the improvement one would achieve by including b-tagging. The solid lines (upper (red) for high and lower (black) for low luminosity) are without b-tagging.

3.2 Systematic Studies

The main source for systematic uncertainty in the pair-production analysis is avoided here by considerably reducing the numerical cut on the number of required jets for an event to be accepted as a signal candidate. A crude evaluation of the expected systematic uncertainty is performed by shifting the cut values by a reasonable amount. These results are summarized in Table 3.

Cut	Cut Value	Change	$\epsilon_{Signal}[\%]$	$N_{Background}$	Significance $[\sigma]$
Σp_t	1200	60	16.8-20.6	12066-17622	32.4-32.9
$p_t(jet5)$	80	4	17.8-19.7	13620-	32.3-
Thrust	0.8	0.050	25.7-11.7	30613-5891	31.2-32.3
Circularity	0.15	0.025	17.8-19.8	13427-16076	32.6-33.1
Nominal Value			18.8	14668	32.9

Table 3: The effect of shifts in the various cut positions on the number of surviving signal and background events. The significance (column 6) is evaluated at point #5 [1]. The values for the p_t cut on the 5^{th} jet is one-sided due to the preselection. The numbers are computed for a luminosity of $1 fb^{-1}$.

Additional systematic error results from the uncertainty on the various internal generator switches e.g. fragmentation and parton shower parameters [7], underlying and minimum bias event parameters [8] and the strong coupling constant (QCDLAM) (Figure 7). All these changes resulted in small effect of the evaluated sensitivity.

An additional test of the stability of the result is obtained by rerunning the signal and background processes with a different generator, namely, Herwig 6.5 for signal and background and Pythia for background. The expected background according to the Pythia generator is $\approx 63\%$ of the one predicted by Herwig 6.4. The Background expectation using Herwig 6.5 is also lower than the one obtained by 6.4, only 78%, but also the signal production cross-section is scaled down. The resulting sensitivity using Herwig 6.5 is therefore almost identical to the one obtained by 6.4.

A similar study was carried out at some of the points which are on the sensitivity curves shown in the figures above. In all of the tested cases the systematic effect was found to be small.

[7] in particular: VQCUT, VGCUT, CLMAX, CLPOW, RMASS(13), SUDORD,INTER, QSPAC, ISPAC, PSPLT, NSTRU were modified.

[8] in particular: PRSOF, ENSOF, PMBN, PMBM and PMBP were modified.

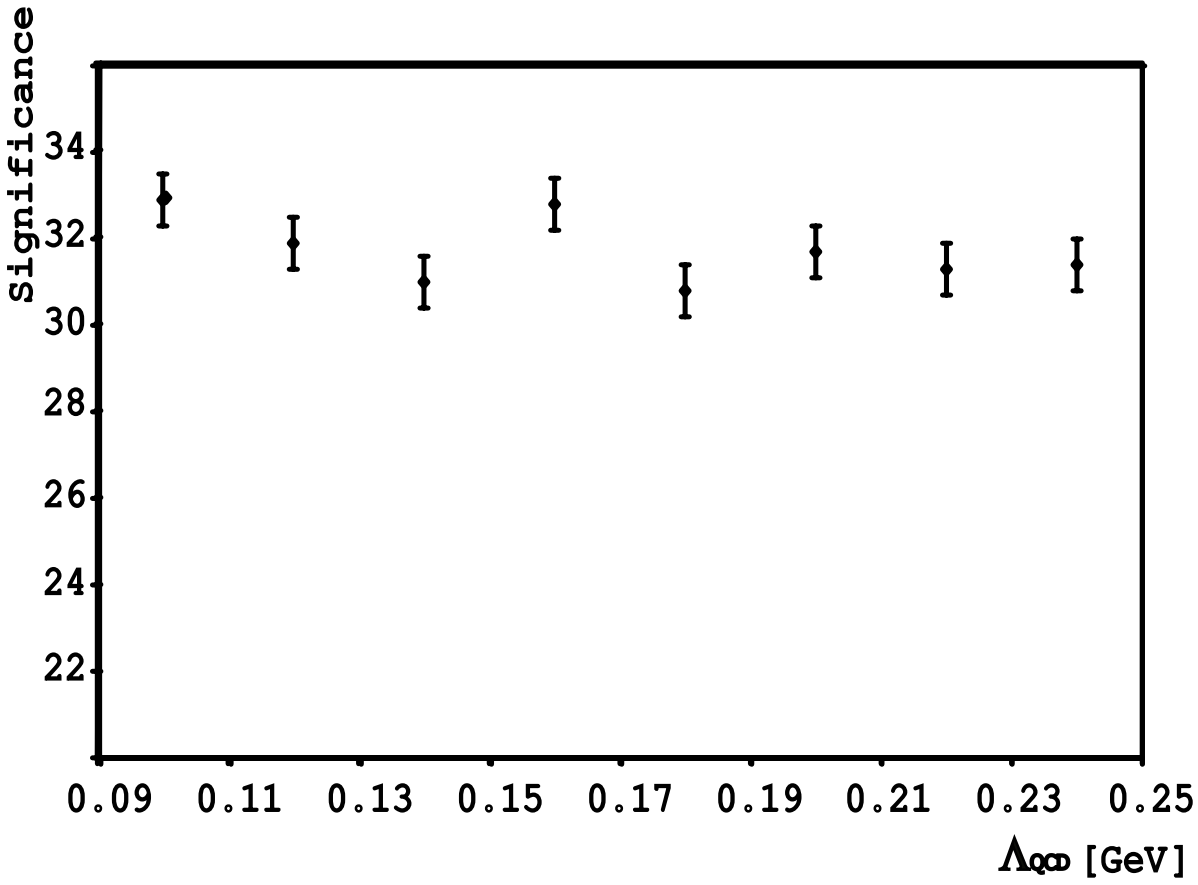

Figure 7: The sensitivity of ATLAS evaluated at point #5 as a function of the value of Λ_{QCD}.

4 Resonance Squark Production

If one of the purely hadronic RPV couplings, λ''_{ijk}, differs from zero, a new SUSY production channel is opened, namely, an *s-channel squark resonant production*. The cross-section for such a process is proportional to $(\lambda''_{ijk})^4$ and will be of interest only if λ''_{ijk} is relatively large.

The experimental signal that one will be searching for is a bump in the reconstructed invariant mass of the events. For low squark masses the QCD background is way too high and a signal cannot be extracted. For high squark masses the signal's production cross-section is below the observable limit. Consequently only if squarks masses are in an intermediate window such a process can give rise to an observable signal.

Signal and background were simulated in a similar way to the one in the previous study, namely, by Herwig 6.4 followed by fast simulation of the ATLAS detector.

Few simple signal selection criteria were applied, namely:

1. $N_{jet} > 1$;
2. $p_t(jet_1) > 800\ GeV$ where $p_t(jet_1)$ is the highest transverse momentum of a jet;
3. Circularity < 0.08: to ensure the right two-jet topology of the events;
4. $M_{12} > 1700\ GeV$ where M_{12} is the transverse mass of the two highest p_t jets.

These cuts practically eliminate all sources of background except the high p_t ($p_t > 800\ GeV$) tail of the QCD processes.

4.1 Optimization of Mass Reconstruction

The sensitivity of the analysis is directly proportional to the quality of the resonance mass reconstruction. Reconstructing the resonance mass from the invariant mass of the two leading jets was found to be a bad choice since in a significant number of events at least one energetic gluon jet was radiated off one of the leading quarks. In order to cope with this phenomena several additional methods have been tried:

- Compute the resonance mass by summing all the observed jets (defined by the standard jet algorithm with a cone of $\Delta R = 0.7$). In order to suppress the effect of the ISR and the underlying event an η and a lower p_t cut on the jets were tried. The former did not improve the performance at all, while the latter resulted in a significant improvement;

- Compute the resonance mass by summing all the calorimeter cells ignoring their jet assignment. A lower p_t cut was tried in order to suppress the destructive effect of the underlying event;

- Compute the resonance mass by tracing two large cones around the two most energetic (p_t) jets. The half-opening angle of these cones was optimized as described below.

- Compute the resonance mass by tracing two large cones around the two most energetic jets provided no additional energetic jet exist. In case such a jet exist - trace 3 cones (provided no fourth energetic jet exist, and so on). Two parameters had to be optimized: the half opening angle and the threshold energy of the additional jet which initiate a cone.

A Gaussian was fit to the mass peak in each of the cases described above and the width of the peak was determined using this Gaussian. Obviously, there were always non-Gaussian tails and the fraction of signal events which falls within a window of $\pm$200 GeV, namely $\pm 2\sigma$ of the best method was also determined. The results are given in Table 4.

	all jets	all cells	two cones	multi cones
σ of peak [GeV]	116	135	99.5	97.2
peak shape	pos. skew	pos. skew	symmetric	symmetric
% in $\pm$ 200 GeV	42.1	39.2	61.0	60.3
parameters		$p_t^{min}(cell) > 4GeV$	ΔR^{cone}=1.5	ΔR^{cone}=1.3 p_t^{min}=200 GeV

Table 4: The results of the resonance reconstruction with the four methods as described in the text.

As can be concluded the best method was the two-large-cone technique which resulted in 5% mass resolution and left more than 60% of the signal inside the mass peak which is shown in Figure 8.

The fact that more than 30% of the signal fell outside of the mass peak prompted a study of the ISR and underlying event in the simulated signal. For this study, Z^0 events in which the Z^0 was forced to decay into a $\nu\bar{\nu}$ final state and in which the mass of the Z^0 was artificially tuned were produced. Since the mass of the produced resonance sets up the scale of the process, the p_t of the ISR jets is affected by it.

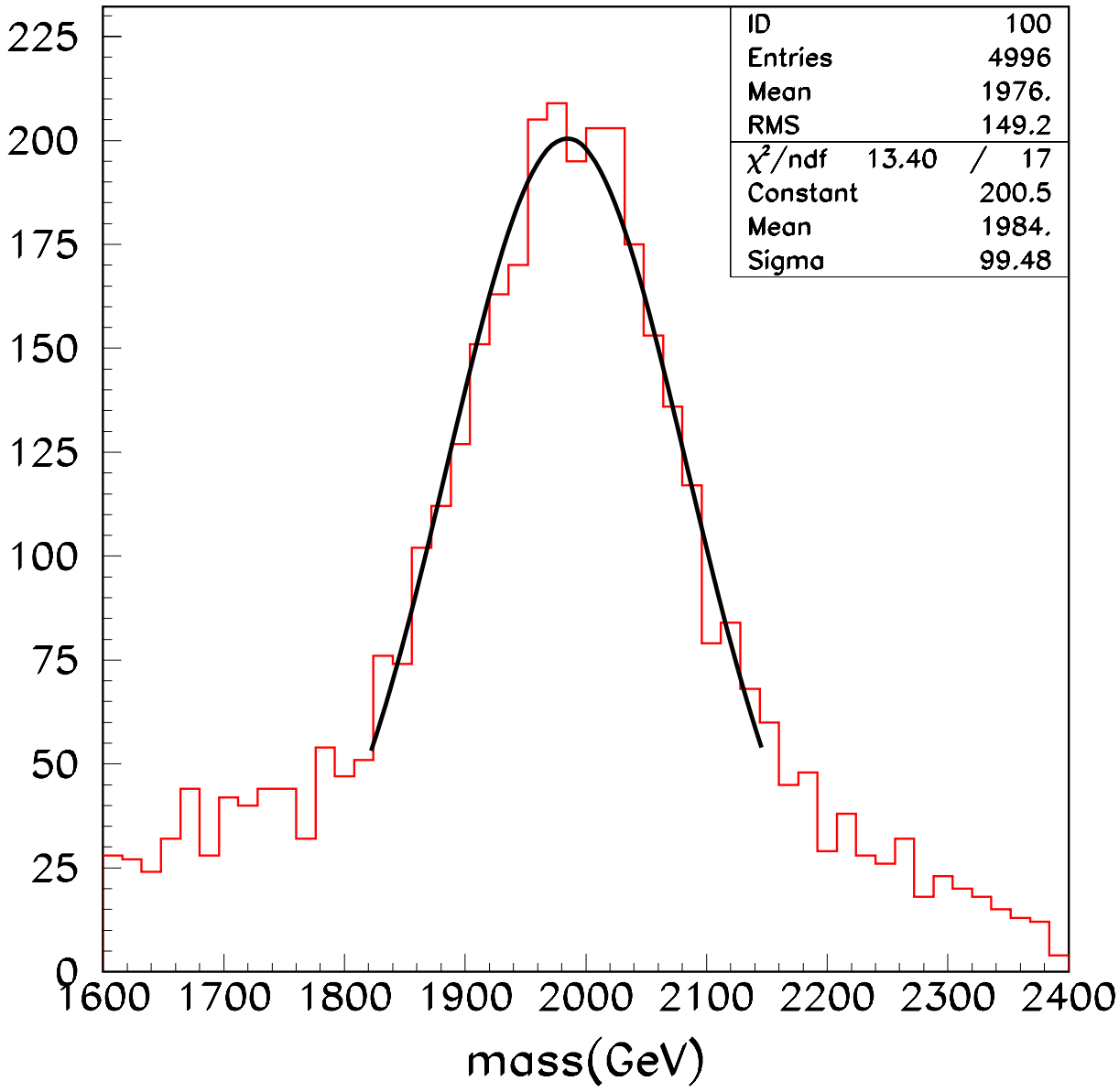

Figure 8: The reconstructed resonance mass using two large cones of half opening angle of $\Delta R = 1.5$. Also shown is the Gaussian fit to the simulated mass distribution.

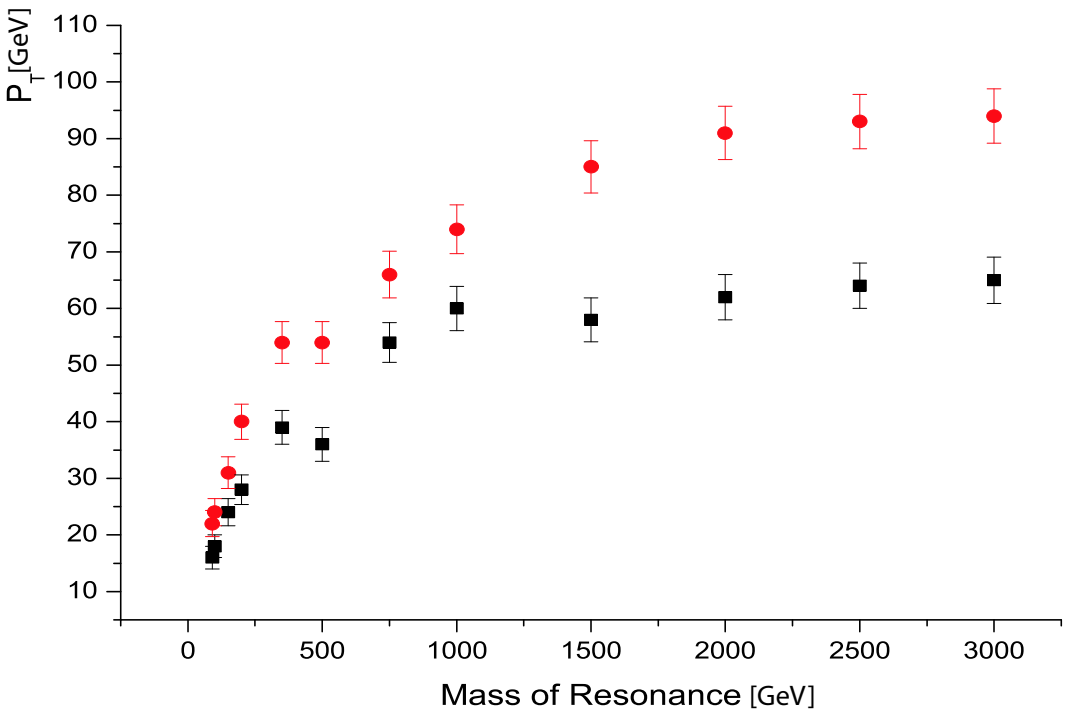

Figure 9: The maximal jet p_t (red) and average p_t of all ISR jets as a function of the mass of the produced resonance. This plot is obtained by running Pythia. Similar behavior is observed while running Herwig with and without Jimmy.

Indeed, the ISR transverse activity was found to increase with the increase of the mass of the produced resonance. The maximal p_t as well as the average p_t of the ISR jets in such events is shown in Figure 9 as a function of the resonance mass.

As was mentioned above, for large values of $\lambda"_{ijk}$ the physical mass of the squark is affected by the inclusion of the RPV couplings in the RGE equations and the squarks tend to be lighter than their computed mass in RPC MSSM. For that reason the interpretation of the results in the $(m_0, m_{1/2})$ plane must be done with the proper tool, namely SOFTSUSY.

The exclusion contours for one of the 9 relevant $\lambda"s$, namely, $\lambda"_{212}$ are shown in Figure 10 for the case of $\mu > 0$, $A_0 = 0$, and $tan(\beta)$=10. Note that the region at high $m_{1/2}$ and low m_0 which is theoretically excluded since the stau becomes the LSP is not excluded in the RPV case.

The dependence of the contour on the value of the relevant $\lambda"_{ijk}$ is shown for one example, namely for $\lambda"_{212}$, $A_0 = 0$, $tan\beta = 10$, μ is positive, $m_0 = 1500$ GeV and

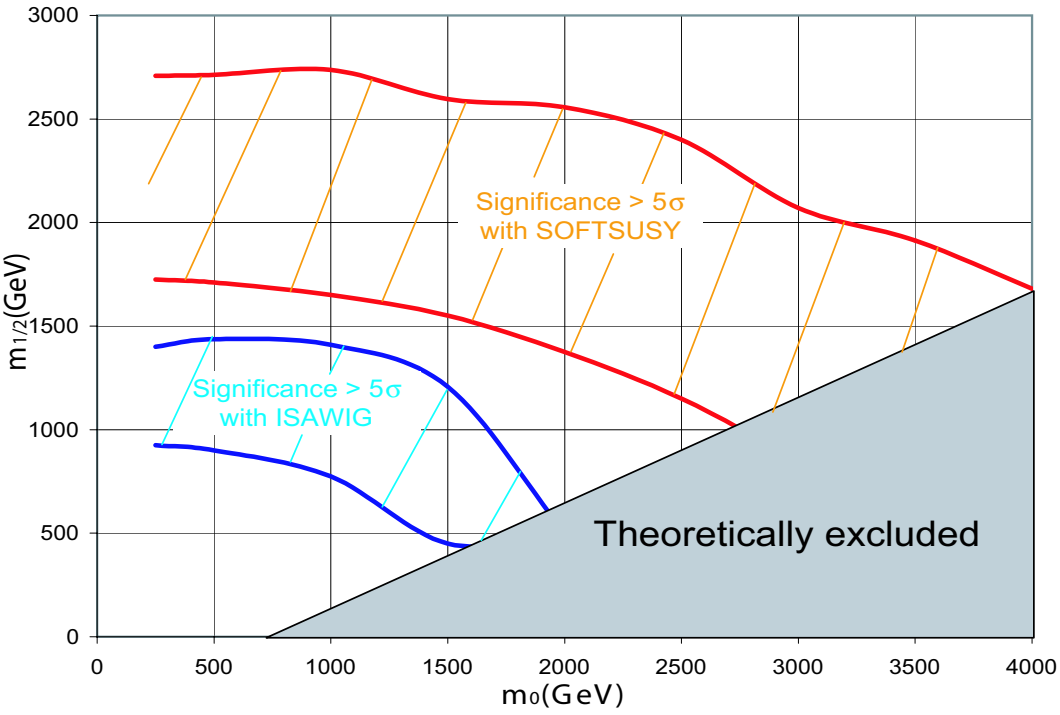

Figure 10: Sensitivity contours for ATLAS resonant squark production. The results are computed for the case in which $A_0 = 0$, $tan\beta = 10$, μ is positive and $\lambda"_{212} = 1$. The figure is drawn for a luminosity of one fb^{-1}.

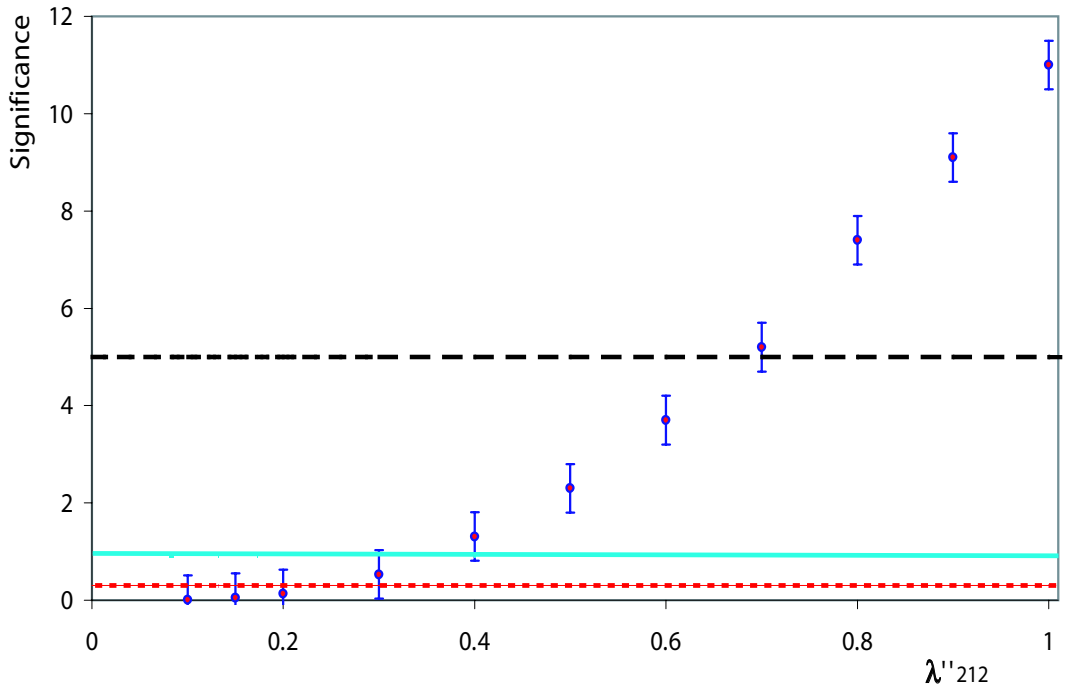

Figure 11: The dependence of the limit on the value of $\lambda"_{ijk}$ for the case of $\lambda"_{212}$, when $A_0 = 0$, $tan\beta = 10$, μ is positive, $m_0 = 1500$ GeV and $m_{1/2} = 750$ GeV. The dashed black line represents the level above which a significance of 5 σ with luminosity of 1 fb^{-1} is reached. The lower solid turquoise line is drawn for a luminosity of 30 fb^{-1} and the lowest dotted red line for a luminosity of 300 fb^{-1}.

$m_{1/2} = 750$ GeV in Figure 11.

4.2 b-tagging

b-tagging can also improve the sensitivity of some signals in the squark resonant production case. Table 5 lists the expected percentage of events containing at least one b-quark jet for the nine possible RPV couplings. The numbers are computed for $m_0 = 2000$ GeV and $m_{1/2} = 300$ GeV squark resonance assuming also that A_0=0, $tan\beta = 5$ and a positive μ. For comparison, the b-quark content in QCD events with $p_t > 500$ GeV is 12.5%. The region in which ATLAS will be able to observe a signal with statistical significance of 5σ after collecting an integrated luminosity of 30 fb^{-1} is shown in Figure 12 for the case of resonating stop, A_0=0, $tan\beta$=10, positive μ and $\lambda"_{313} = 1$. The improvement achieved by adding b-tag to the other cases (except for the $\lambda"_{323} = 1$ one) is marginal.

Coupling	b-percentage
λ''_{112}	4.3%
λ''_{113}	15.4%
λ''_{123}	33.5%
λ''_{212}	3.6%
λ''_{213}	42.9%
λ''_{223}	50.9%
λ''_{312}	2.9%
λ''_{313}	95.4%
λ''_{323}	95.2%

Table 5: The percentage of b-flavored events for various RPV couplings

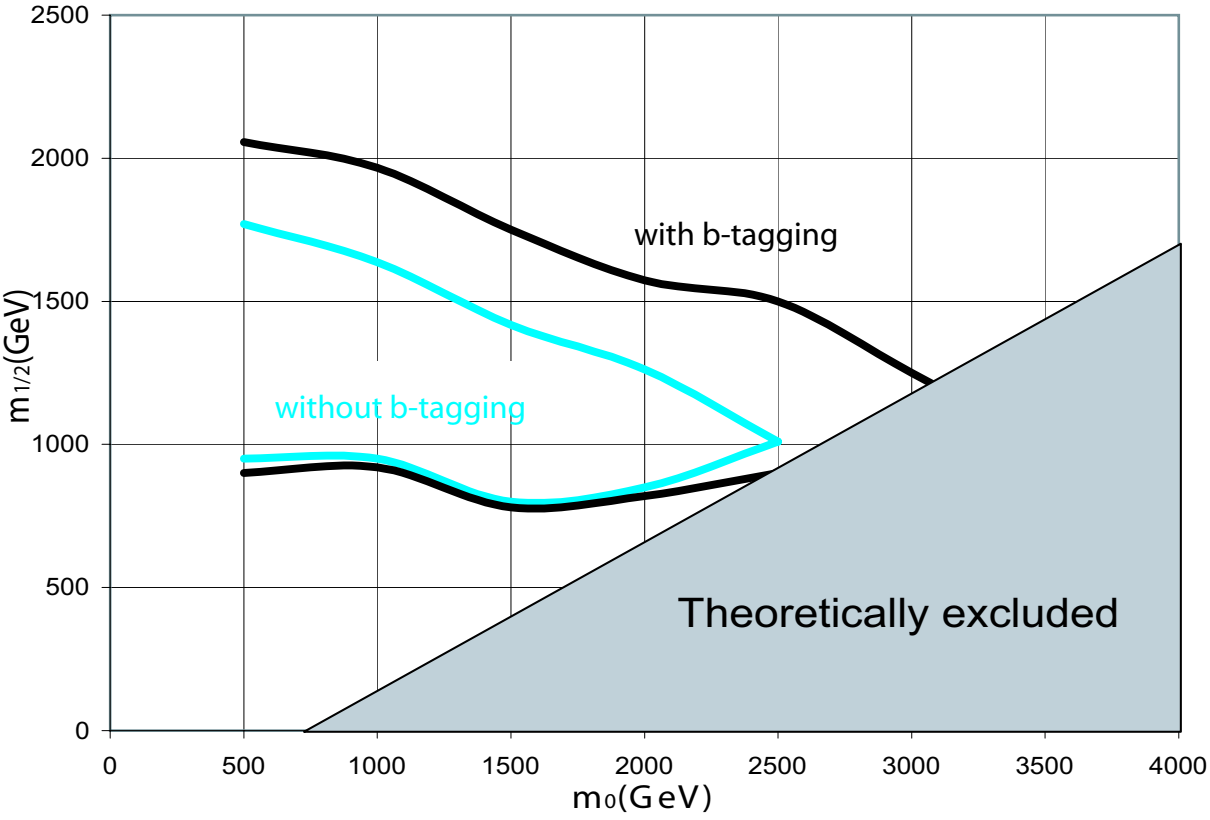

Figure 12: Sensitivity contours for ATLAS resonant stop production with and without b-tagging. The contours represent the 5 σ ones attainable with integrated luminosity of $30 fb^{-1}$.

4.3 Systematic Uncertainties

The standard way of shifting the cutoff values has been applied and the results are shown in Table 6. The numbers were evaluated for m_0=1500 GeV, $m_{1/2}$=750 GeV, A_0=0, $tan\beta$=10, $\mu > 0$ and for $\lambda''_{212} = 1$. The effect of changing the cuts, as one can clearly see, is quite small.

Cut	Cut value	Change	$\epsilon_{signal}[\%]$	$N_{background}$	Significance $[\sigma]$
p_t^{jet1}	800 GeV	40 GeV	24.9-24.9	6247-6251	11.1-11.1
m_t^{2-jets}	1700 GeV	85 GeV	19.8-29.1	4130-8616	10.9-11.0
Circularity	0.08	0.004	24.9-24.8	6265-6226	11.1-11.1
mass window	300 GeV	15 GeV	25.4-24.3	6528-5946	11.1-11.1
nominal value			24.9	6249	11.1

Table 6: The systematic effect of a 5% shift in the cutoff value of the various cuts used in the analysis. The numbers are computed for a luminosity of one fb^{-1}.

The uncertainty on the exact value of the strong coupling constant might result in a large effect in this analysis. In Figure 13 the dependence of the statistical significance of the analysis at the above mentioned point is shown as a function of Λ_{QCD}. Again, the effect is very small.

Hence, one may conclude that the systematic uncertainty of the contour plots shown in this section are quite small. However, the computations described above are based on fast detector simulation and relay on the present parton-shower event generators that do not take NLO corrections into account. Is is now known [13] that these generators underestimate the level of expected SM background in comparison with Matrix Element generators (e.g. Alpgen [14]). Hence, the actual uncertainly might be considerably larger and the sensitivity somewhat lower.

5 Conclusion

A new analysis for the search of sparton pair production followed by their RPV decay was presented. This analysis does not rely on requiring a large number of jets in the final state and its background estimation is therefore more reliable. ATLAS will be sensitive to MSSM signals if $m_{1/2}$ is bellow $\approx$ 500 GeV and m_0 is bellow 1000 GeV with just $1fb^{-1}$. For low values of m_0 the sensitivity is dropping. Including b-tagging the sensitivity is somewhat enhanced (up to $m_{1/2} \approx$ 550 GeV).

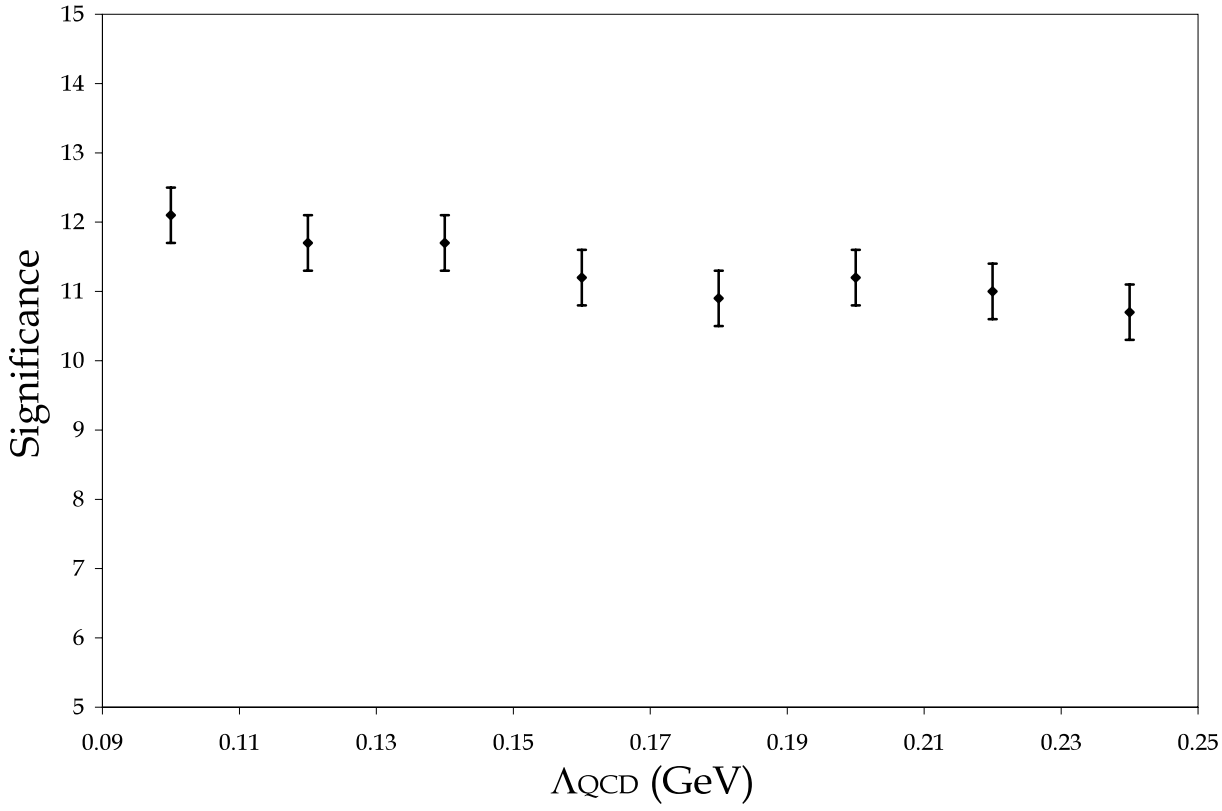

Figure 13: The dependence of the statistical significance of the analysis at the above mentioned point is shown as a function of Λ_{QCD}.

Another analysis, in which a resonating squark is produced and disintegrates through the RPV coupling is also studied. This channel is visible if the relevant $\lambda"_{ijk}$ is relatively large, i.e. at least 0.3. The signal at low masses is invisible due to QCD background and will be seen as a mass peak only for very large MSSM parameters, namely, when both $m_{1/2}$ and m_0 are in the 1000-2000 GeV region.

6 Acknowledgments

We would like to thank the members of the Weizmann group: Eilam Gross, Peter Renkel, Michael Riveline and Lidija Zivkovic for their help in discussing the various aspects of the present work. We are obliged to the Benoziyo center for High Energy Physics for their support of this work. This work was also supported by the Israeli Science Foundation(ISF) and by the Federal Ministry of Education, Science, Research and Technology (BMBF) within the framework of the German-Israeli Project Cooperation in Future-Oriented Topics(DIP).

References

[1] ATLAS Collaboration, TDR 2, CERN LHCC/99-15, 811-914.

[2] Consequences of Baryonic R-parity Violation for Measurements of SUSY Particles using the ATLAS Detector, J.Soderqvist, ATL-PHYS-98-122.

[3] Study of the determination of the SUGRA parameters using the ATLAS detector in the case of L-violating R parity breaking, A.Mirea; E.Nagy, HEP-PH/9904354, ATL-PHYS-99-007.

[4] Measurement of the LSP mass in supersymmetric models with R-parity violation, L.Drage; M.A.Parker, ATL-PHYS-2000-007.

[5] Measuring Supersymmetric Particle Masses at the LHC in Scenarios with Baryon-Number R-Parity Violating Couplings, B.C.Allanach; A.J.Barr; L.Drage; C.G.Lester; D.Morgan; M.A.Parker; P.Richardson; B.R.Webber, JHEP 0103 (2001) 048, HEP-PH/0102173, ATL-PHYS-2002-002.

[6] Extracting the Flavour Structure of a Baryon-Number R-parity Violating Coupling at the LHC, B.C.Allanach; A.J.Barr; M.A.Parker; P.Richardson; B.R.Webber, JHEP 0109 (2001) 021, HEP-PH/0106304, ATL-PHYS-2002-003.

[7] Signals from R-parity violating top quark decays at LHC, A.Belyaev; M.H.Genest; C.Leroy; R.Mehdiyev, JHEP 0409 (2004) 012, HEP-PH/0401065, SN-ATLAS-2004-039.

[8] B.C. Allanach et al., HEP-PH/9906224.

[9] G. Corcella et al., JHEP 0101 (2001) 010, HEP-PH/0011363 and HEP-PH/0210213.
S. Moretti et al., JHEP 0204 (2002) 028, HEP-PH/0204123.

[10] Pythia 6.2 Physics and Manual, T.Sjostrand; L.Lonnblad; S.Mrenna; P.Scands HEP-PH/0108264, LU-TP 01-21 (2002).

[11] B.C. Allanach et al., Phys.Rev. D69 (2004) 115002, HEP-PH/0309196.
B.C. Allanach, Comput. Phys. Commun. 143 (2002) 305-331, HEP-PH/0104145.
E. Duchovni, A. Melamed-Katz and R. Feldesh, Note in preparation.

[12] M. Spiropulu, EFI-01-23,FERMILAB-Conf-01/110-E, HEP-EX/0106045.

[13] S. Asai, Talk at the 4^{th} ATLAS Physics Workshop, Rome, June 2004.

[14] M. L. Mangano, F. Piccinini, A. D. Polosa, M. Moretti, R. Pittau, CERN-TH/2002-129 hep-ph/0206293